ELSEVIER

Journal of Fluids and Structures 18 (2003) 741–758

JOURNAL OF FLUIDS AND STRUCTURES

www.elsevier.nl/locate/jnlabr/yjfls

Vortex-shedding from single and tandem cylinders in the presence of applied sound

J.W. Hall*, S. Ziada, D.S. Weaver

Department of Mechanical Engineering, McMaster University, 1280 Main Street West, Hamilton, Ont., Canada L8S 4L7

Received 17 February 2003; accepted 6 June 2003

Abstract

A single cylinder and two tandem cylinder configurations with longitudinal pitch ratios $L/D = 1.75$ and 2.5 were rigidly mounted in an open circuit wind tunnel and a standing acoustic pressure wave was imposed so that the acoustic particle velocity was normal to both the cylinder axis and the mean flow velocity. The effect of sound on the vortex-shedding was investigated for various amplitudes by means of pressure taps on the cylinders and wake hot-wire probes. These tests show that applied sound can entrain and shift the natural vortex-shedding frequency to the frequency of excitation and produce nonlinearities in the wake. The lock-in envelope for the tandem cylinders is considerably larger than for the single cylinder. The lock-in range for the smaller tandem cylinder spacing was broader still than either the single cylinder, or the $L/D = 2.5$ tandem cylinder case. The pressure and hot-wire measurements show for the single cylinder, and tandem cylinder configuration with pitch ratio $L/D = 2.5$, that there was a phase jump near the coincidence of the vortex-shedding frequency and the excitation frequency, while there was no jump for the pitch ratio of 1.75. As well, the applied sound field was also noted to induce vortex-shedding in the gap for the $L/D = 2.5$ case, while no vortex-shedding was noted for the smaller pitch ratio.

1. Introduction

It is well known that vortex-shedding in the wake of a cylinder produces fluctuating lift and drag forces on the cylinder, and should the vortex-shedding frequency be sufficiently close to the natural frequency of the cylinder, the induced motion can fully correlate the vortex-shedding along the cylinder span. This can produce large fluctuating lift forces and can cause structural damage. The process of bluff body motion entraining vortex-shedding is known as lock-in. This phenomena has received much attention in the literature [see the review of Bearman (1984) for example], and its study typically takes one of two forms, either the self-excited vibration of a flexible cylinder is investigated and the amplitude is damping dependent [e.g. Feng (1968)], or the cylinder is forced to oscillate transversely at a sufficient amplitude that the wake is locked-in [e.g., Bearman and Currie (1979)].

Blevins (1985) showed an applied sound field can induce a locked-in wake for a rigid, stationary cylinder. He used electromagnetic speakers to excite an acoustic standing wave in a wind tunnel test-section where the acoustic field was oriented such that the acoustic particle motion was normal to the mean flow velocity and the cylinder axis. He showed that the sound field could shift and entrain the vortex-shedding to the frequency of excitation and could fully correlate the vortex-shedding along the cylinder span. In effect, Blevins performed a forced vibration experiment where rather than oscillate the cylinder, the surrounding fluid was oscillated. The aim of the present study is to assess the effect that acoustic excitation has on vortex-shedding from multiple bluff body configurations. This study will focus on the simplest configuration, a two cylinder tandem arrangement, as shown in Fig. 1.

*Corresponding author. Tel.: +1-905-525-9140; fax: +1-905-572-7944.
E-mail address: halljw@mcmaster.ca (J.W. Hall).

0889-9746/$ - see front matter © 2003 Elsevier Ltd. All rights reserved.
doi:10.1016/j.jfluidstructs.2003.06.003

Nomenclature

A	peak amplitude of cylinder displacement
c	speed of sound
D	cylinder diameter
f_o	frequency of vortex-shedding in absence of excitation
f_e	frequency of excitation
i	complex number, $\mathrm{i} = \sqrt{-1}$
l	mode number: 0,1,2…
L	streamwise cylinder spacing
m	mode number: 0,1,2…
P_d	pressure measured on downstream cylinder pressure tap
P_u	pressure measured on upstream cylinder pressure tap
P_{wall}	pressure measured at test-section wall
t	time
U	upstream flow velocity
v_c	peak velocity of cylinder vibration
v_p	peak acoustic particle velocity
x	streamwise coordinate
$\hat{\mathbf{x}}$	streamwise unit vector
y	transverse coordinate
$\hat{\mathbf{y}}$	transverse unit vector

Greek letters

ζ	peak acoustic particle displacement
v	kinematic velocity
ρ	ambient fluid density
Φ	phase angle

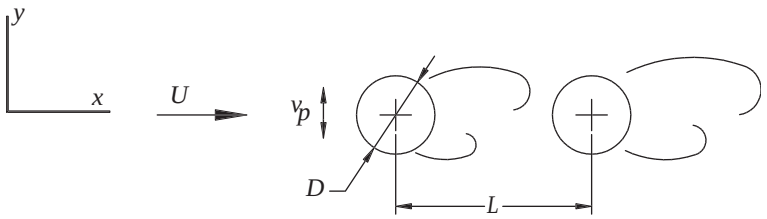

Fig. 1. The tandem cylinder system.

Zdravkovich (1977, 1987) reviewed and classified the flow over tandem cylinders. For pitch ratios in the range $1 < L/D < 1.3$–1.8, the cylinders behave as a single bluff body and the shear-layers shed from the front cylinder do not reattach onto the second cylinder. In the range 1.2–$1.8 < L/D < 3.4$–3.8, the shear-layers shed from the first cylinder reattach to the face of the secondary cylinder and vortex-shedding occurs only in the wake of the second cylinder. For pitch ratios above this, vortex-shedding occurs both in the gap formed between the cylinders and behind the second cylinder. The exact spacing at which regime transitions occur is also somewhat dependent on Reynolds number.

Mahir and Rockwell (1996) performed forced-vibration tests on a single cylinder and on two different tandem cylinder configurations, namely $L/D = 2.5$ and 5.0. Both cylinders were mechanically oscillated normal to the cylinder axis and the mean flow velocity. The apparatus allowed the cylinders to be oscillated at variable phase angles to one another, although only the case where the two cylinders are oscillated in phase, similar to the present experiments is considered here. They showed that the breadth of the lock-in range for the $L/D = 5.0$ case was quite similar to that of a single cylinder, while the sub-critical pitch ratio $L/D = 2.5$, had a considerably wider lock-in range. They attributed this

behaviour to the stagnant gap flow region that exists between the cylinders. They also observed that the vortex-shedding could be entrained at approximately half the amplitude of the single cylinder case.

The present experimental investigation will examine the effect of varying the proximity of the two cylinders on the flow-acoustic coupling. In particular, two subcritical pitch ratios were examined so that the unusual behaviour observed by Mahir and Rockwell (1996) could be further investigated. The tandem cylinder configuration with pitch ratio $L/D = 2.5$ was chosen for comparison to Mahir and Rockwell (1996), and a smaller pitch ratio, $L/D = 1.75$, was also examined. Similar experiments were also performed on a single cylinder in an applied acoustic field. In the present investigation, the flow is examined in the presence and absence of an applied sound field. External acoustic excitation of controlled amplitude, and frequency f_e, is applied such that the acoustic particle velocity, v_p, is in the direction normal to the cylinder axis and the mean flow velocity. This is the same as in the usual flow-excited acoustic resonance in a duct and is similar to Blevins (1985). The direction of the acoustic particle velocity relative to the cylinders is shown in Fig. 1.

A description of the experimental set-up and procedure is outlined, followed by the results for the single cylinder and the two, tandem cylinder configurations in the absence of an externally applied sound field. The results obtained with the application of an external sound field are then presented and the results are discussed. The present paper will summarize and expand the two previous works by Hall et al. (2002a, b).

2. Experimental set-up

2.1. Single cylinder tests

The cylinder was rigidly mounted to eliminate the possibility of any vibration, and spanned the shorter dimension of a 711 mm × 216 mm rectangular wind-tunnel test-section as shown in Fig. 2. The test-section was mounted on the exhaust end of an open circuit wind tunnel and was constructed out of 11.9 mm plywood. This facility provided a maximum flow velocity of approximately 30 m/s and a streamwise turbulence intensity of less than 0.5%.

The test cylinder was machined from solid aluminium and was polished smooth to be free of any surface defects. Both ends of the cylinder were drilled and tapped to facilitate bolting it rigidly to the test-section walls. In order to achieve coincidence of the vortex-shedding frequency f_o, with the duct acoustic natural frequency f_e, a 1.27 cm diameter cylinder was used. The aspect ratio for this set-up was 17, and consequentially the solid blockage was only 2%. Although no measurements of the correlation of the flow along the cylinder axis were taken, the literature [e.g. Norberg (2003)], suggests that the correlation length should be approximately $4D$ with no sound applied, and there should be roughly four correlated vortex cells at any given instant. In the presence of applied sound Blevins (1985) showed that the vortex-shedding from a single cylinder became fully correlated along the span of the cylinder, essentially forcing the vortex-shedding to become two-dimensional. Thus in the present study the cylinder is long enough so that the flow is appropriately three-dimensional before sound is applied, and the presence of the applied sound field forces the flow to become increasingly two-dimensional.

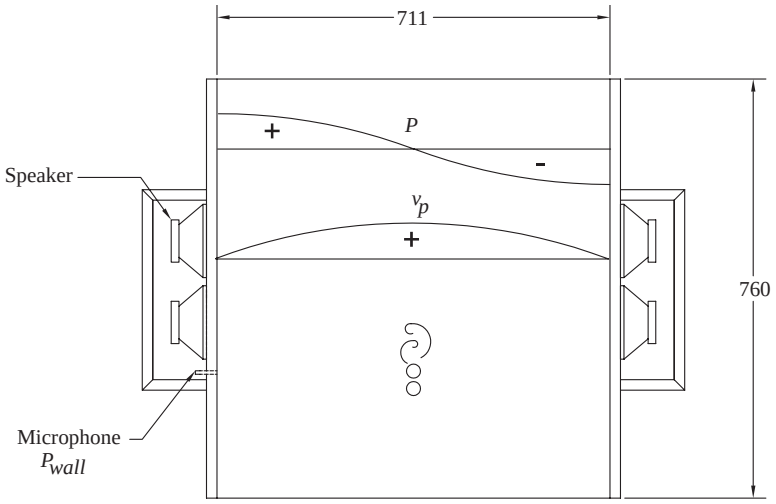

Fig. 2. Plan view of wind tunnel test-section. All dimensions are in mm.

A 0.40 mm diameter hole was drilled at the midspan of the cylinder to allow dynamic pressure measurements to be made at the cylinder surface. This was connected to a 6.35 mm condenser microphone via a 3.18 mm diameter hole bored through the cylinder. The microphone was mounted and sealed into a specially modified bolt used to affix the cylinder. The acoustic natural frequency of the pressure tap system was experimentally determined to be 750 Hz, considerably higher than any frequencies of interest in the present experiments. Any system such as this will impose an inherent time lag between when the signal arrives at the surface of the cylinder and when the microphone receives the signal. Subsequent experiments revealed that this phase lag was 55° at the frequency of acoustic excitation, and all pressure tap measurements were corrected by this value. As will be shown, an acoustic pressure node exists at the cylinder location, thus the pressure tap is primarily measuring the fluctuating pressure associated with the vortex-shedding and not the acoustic pressure.

For the single cylinder experiments the pressure tap was oriented so that it was rotated 80° from the front stagnation point of the cylinder as shown in Fig. 3. Lee and Panagakos (1997) showed this to be the approximate separation point for a single cylinder in the absence of applied sound. This was confirmed by physically rotating the cylinder and examining the amplitude of the signal in the absence of an external sound field.

A hot-wire probe placed one diameter downstream of the cylinder was used to ascertain the vortex-shedding frequency and consequently the presence of lock-in. The position of the roving wire is shown in Fig. 3. Because the wake width of the cylinder can vary with Reynolds number and amplitude of acoustic excitation, this probe could be traversed across the wake. To obtain the signal, the wire was traversed just outside of the wake until a clean, sinusoidal signal was obtained. This ensured that the wire was outside the turbulent wake region where the mean flow velocity is low, and thus the hot-wire is measuring the wake response and not the acoustic particle velocity.

In order to quantify the magnitude of the acoustic standing wave, a 6.35 mm GRAS 40BP condenser microphone was flush-mounted on the test-section sidewall as shown in Fig. 2. This pressure measurement allowed the acoustic particle velocity v_p, and acoustic particle displacement ζ, at the cylinder location to be calculated.

A 16 Bit, simultaneous sampling, data acquisition system was used to digitize the aforementioned signals. The data acquisition system was equipped with onboard filters to prevent aliasing. All data was collected and processed online and individual power-spectra were computed for each signal. Cross-spectra referenced to the test-section wall microphone were computed for the pressure-tap and stationary hot-wire signals allowing the phase angle Φ, to be measured at f_e. All signals were sampled at 4096 Hz and each individual block was collected for a 1 s duration yielding a spectral resolution of 1 Hz. All spectra are a result of 100 averages using a flat-top window.

To excite the acoustic standing wave, two pairs of Rockford–Fosgate speakers were mounted on either side of the test-section and powered using a 200 W per channel Ramsa WP-1200 amplifier. Each speaker pair was connected out of phase on either side of the section, and was covered with a perforated plate, flush-mounted to the inner wall of the section. This reduced the chance of flow separation across the face of the speaker. The speakers were placed in sealed boxes, and were vented to the inside of the test-section reducing the potential for fluid loading on the face of the speakers. The signal was produced using the source from a HP dynamic signal analyser. Using the present configuration the maximum sound pressure level (SPL) that could be produced in the wind-tunnel test-section was approximately 150 dB (ref 20 μPa).

Measurements of the acoustic pressure at the test-section wall P_{wall}, were used to calculate the magnitudes of v_p and ζ using formulae derived in the appendix. This allowed measurements of the phase of the vortex-shedding process to be referenced to ζ, analogous to the practice of referencing local flow properties such as fluctuating lift force to cylinder position in forced-vibration experiments (see Bearman and Currie, 1979, for example).

In the present experiment the excitation frequency, f_e, is set and f_o is varied by changing the mean flow velocity U, though in a typical forced vibration experiment the mean flow velocity is held constant and the amplitude of vibration A, is varied. In the present experiments the magnitude of the excitation was quantified using acoustic particle velocity, nondimensionalized by the mean flow velocity, v_p/U, partially because this measure takes the variation in mean flow velocity into account. The velocity ratio v_p/U is essentially a measure of the incident angle of the flow.

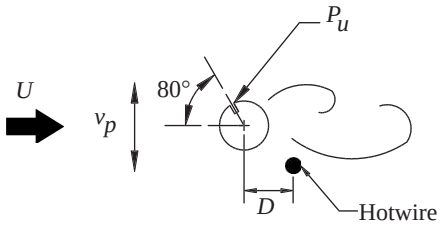

Fig. 3. Single cylinder instrumentation location.

2.2. Tandem cylinder tests

Tests were also performed on a pair of tandem cylinder systems with longitudinal pitch ratios of $L/D = 1.75$ and 2.5. The instrumentation used for these tests was quite similar to the single cylinder tests, and is shown in Fig. 4. An identical second cylinder was rigidly mounted directly downstream of the first cylinder and was also equipped with a pressure tap. The upstream cylinder pressure tap P_u, was oriented at 70° from the front stagnation point, since Arie et al. (1983) showed that this was the approximate upstream cylinder separation point for a tandem cylinder system with a pitch ratio of $L/D = 2$. They also found that the shear layer reattachment point onto the second cylinder face was at approximately 60° from its front stagnation point, and consequently the pressure tap on the downstream cylinder P_d, was set to this angle. Preliminary experiments performed by rotating the pressure tap on the rear cylinder in the absence of the applied sound field for both pitch ratios show a local maximum in the pressure fluctuations on the front face of the rear cylinder at this approximate location. This indicates that the shear-layers shed from the front cylinder are reattaching onto the face of the second cylinder for both tandem cylinder configurations investigated. As well, a stationary hot-wire probe was used to further monitor the vortex-shedding and was mounted as shown in Fig. 4 so that it could measure the enveloped flow created by both the gap flow and the wake.

Flow visualization was also performed on the tandem cylinder configurations. The present technique uses the acoustic pressure signal at the test-section wall to trigger a strobe and by using an adjustable phase delay, any instant of the acoustic cycle could be visualized. A black and white CCD camera was used to record the images on a VCR and monitor system. Because of the capture rate of the camera, each photograph represents an average of nine locked-in vortex-shedding cycles. Smoke was bled in from a commercial fog generator through small holes drilled in the surface of the cylinder, and the gap and wake flow were each visualized separately. It should be noted that a technique such as this is limited to visualizing flow phenomena at integer multiples of the excitation frequency.

2.3. Experimental procedure

The mean flow velocity was set and tests were first performed with no applied sound field. The natural frequency of vortex-shedding was determined from the spectral peak of the roving hot-wire signal. The input signal to the amplifier was then adjusted to a preset ratio of particle velocity to mean flow velocity, v_p/U, by using the pressure spectra taken from the microphone mounted at the test-section wall. The signal was subsequently shut off and the experiment was repeated for a different value of v_p/U. No vortex-induced acoustic resonance was detected at any time, so shutting the sound off between trials ensured no hysteretic effects were present. After the completion of a set of tests, the mean flow velocity was increased and the tests were repeated. For more details on the experimental set-up and procedure see Hall (2001).

3. Experimental results

3.1. No applied sound

The single cylinder was tested for Reynolds numbers based on the cylinder diameter, Re_D, from 12 000 to 17 000. Typical spectra obtained from the hot-wire probe and the pressure tap are shown in Figs. 5 and 6, plotted along with the

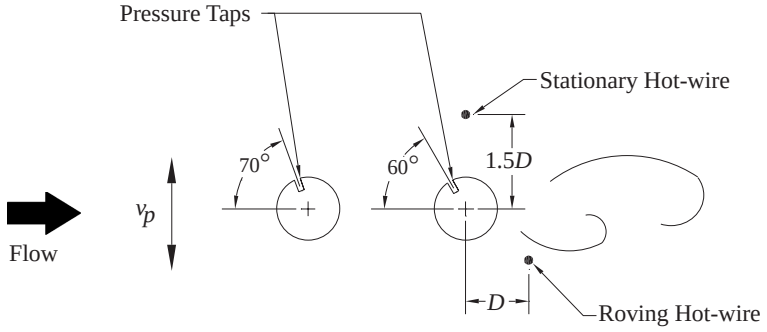

Fig. 4. Tandem cylinder instrumentation location.

spectra obtained in the presence of applied sound. All spectra in the absence of the applied sound field were dominated by a peak at the vortex-shedding frequency (f_o) and although not shown, the harmonic ($2f_o$).

The vortex-shedding frequency measured at each flow velocity is plotted in Fig. 7 in terms of Strouhal number

$$\mathrm{St}(D) = f_o D/U, \tag{1}$$

as a function of Reynolds number Re_D. The present notation is used for reasons that will become apparent in the experiments with applied sound. It is clear that for the single cylinder, the Strouhal number is approximately 0.2, and does not change appreciably with Reynolds number. This value is in good agreement with the generally accepted value of $\mathrm{St}(D) \sim 0.2$ for a single cylinder.

Each of the tandem cylinder systems were tested for Reynolds numbers ranging from 7000 to 24 000. Sample spectra obtained from all instrumentation in the absence of applied sound are shown in Figs. 8 and 9, plotted with spectra obtained in the presence of an applied sound field. The spectra for the tandem cylinder configurations in the absence of excitation are similar to the single cylinder showing a large peak at f_o. For the tandem cylinders studied, f_o does not necessarily increase linearly with flow velocity. This is reflected in Fig. 7 by $\mathrm{St}(D)$ varying with respect to Re_D. Comparisons are also made in Fig. 7 with tandem cylinder data from the literature for similar pitch ratios and Reynolds numbers. The majority of the data shows that the Strouhal number tends to decrease as Reynolds is increased, similar to the results obtained here.

3.2. The effect of acoustic excitation

Tests were performed for six different ratios of dimensionless acoustic particle velocity, v_p/U, for each flow velocity, namely 0.33%, 0.65%, 1.29%, 2.57%, 3.86% and 5.15%. Due to limitations in the speaker power, tests at $v_p/U = 5.15\%$ could only be performed up to a velocity of 23 m/s. Measurements in the presence of the applied sound field were performed for both the single cylinder and the tandem cylinder configurations. The flow velocity ranges tested were dependent on the breadth of the flow entrainment window, and consequently the single cylinder was tested for a much smaller Re_D range than the tandem cylinders.

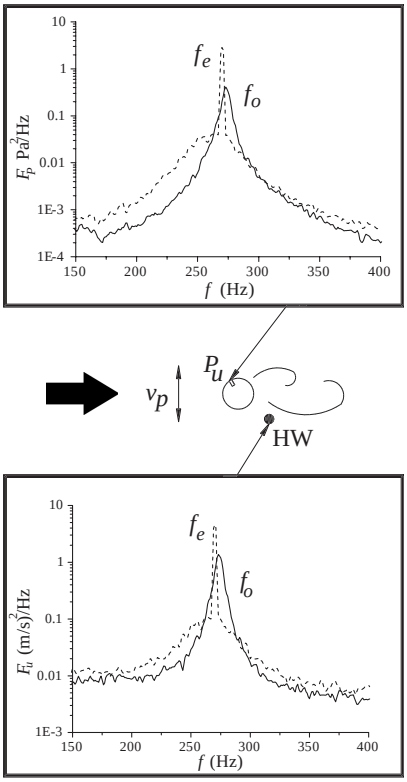

Fig. 5. Spectra taken from the pressure tap and roving hot-wire for single cylinder showing flow entrainment caused by sound, $\mathrm{Re}_D = 14\,400$ and $f_o/f_e = 1.01$: ——, no applied sound; - - -, $v_p/U = 5.15\%$.

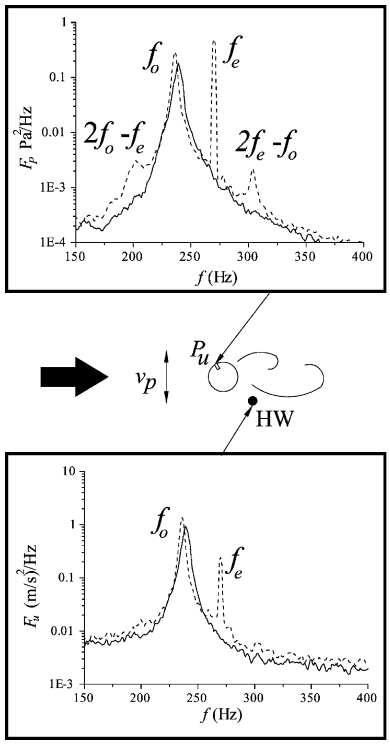

Fig. 6. Spectra taken from the pressure tap and roving hot-wire for single cylinder showing nonlinearities in spectra, $\mathrm{Re}_D = 12\,300$ and $f_o/f_e = 0.89$: ——, no applied sound; - - -, $v_p/U = 1.29\%$.

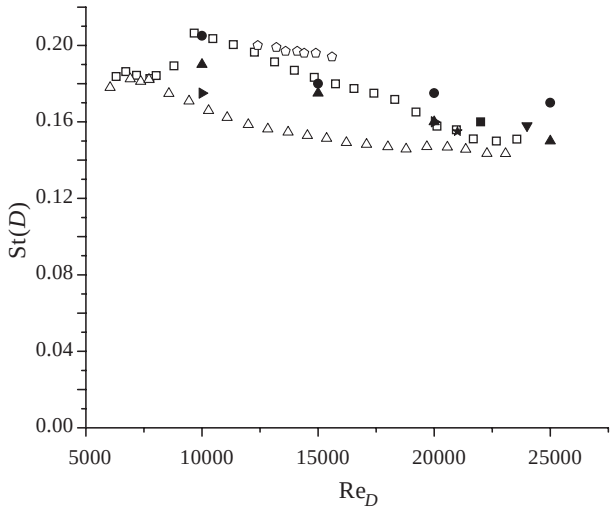

Fig. 7. Comparison of present Strouhal number values in absence of excitation to literature values. Present study: □, $L/D = 1.75$; △, $L/D = 2.5$; ⬠, single cylinder. Igarashi (1981): ▶, $L/D = 2.5$; ▩, $L/D = 1.75$; ●, $L/D = 1.91$; ▲, $L/D = 2.06$. Lee and Basu (1997): ▼, $L/D = 2.0$. Lee and Panagakos (1997): ★, $L/D = 2.00$.

Fig. 5 shows spectra obtained from the pressure tap and the roving hot-wire probe, both in the presence and absence of an applied sound field. It is apparent that the applied sound field shifts the vortex-shedding frequency f_o, to the frequency of the applied sound f_e. As well, it narrows the vortex-shedding peak and increases its magnitude. These are similar to the flush film anemometer results reported by Blevins (1985).

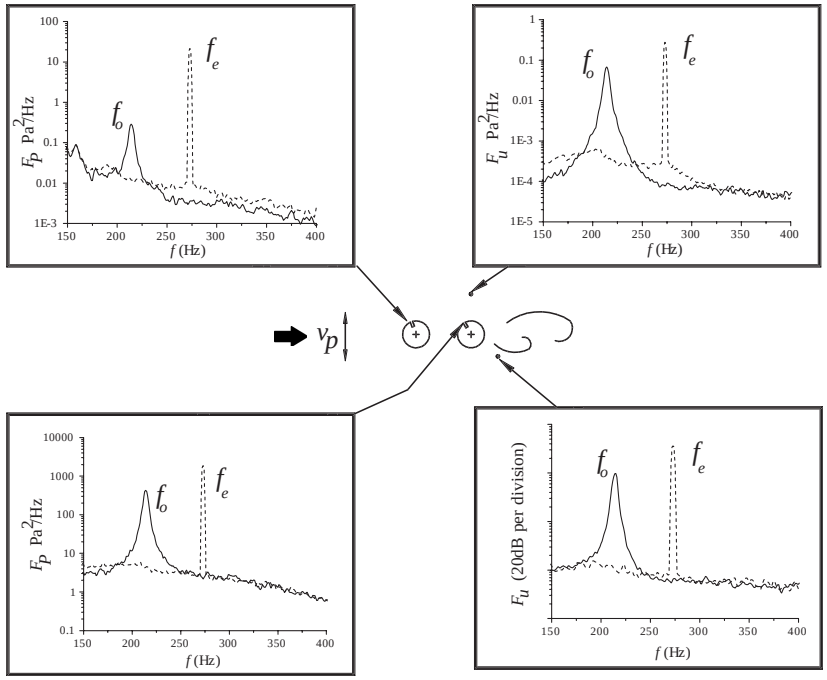

Fig. 8. Effect of applied sound on vortex-shedding from a tandem cylinder system showing locked-in state for $L/D = 2.5$, and $f_o/f_e = 0.80$, —, no applied sound; - - -, $v_p/U = 5.15\%$.

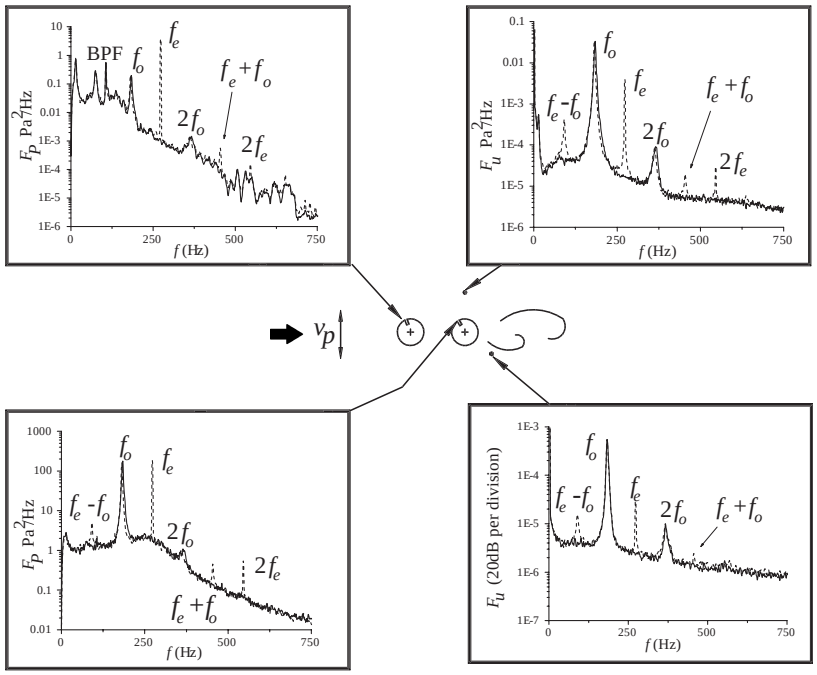

Fig. 9. Effect of applied sound on vortex-shedding from a tandem cylinder system showing nonlinearities in the flow for $L/D = 2.5$, and $f_o/f_e = 0.69$; —, no applied sound; - - -, $v_p/U = 1.29\%$.

Fig. 6 shows that sound can also produce nonlinearities in the wake response similar to those observed by Mahir and Rockwell (1996) in forced-vibration experiments. They showed that if the wake was not locked-in, yet f_o is sufficiently close to f_e, the wake spectra have peaks at linear combinations of the excitation and natural vortex-shedding frequency, such as $f_e - f_o, f_e + f_o, f_o - 2f_e$, and $f_o + 2f_e$. Fig. 6 shows that when sound is applied the wake is clearly not locked-in, but small peaks exist at $2f_o - f_e$ and $2f_e - f_o$. Interestingly, there is little evidence of these peaks in the hot-wire spectra. As well, it should be noted that even when not locked-in there is evidence of the excitation frequency in the shear layers. The nonlinear mechanism that generates these frequency components has been discussed in some detail by Miksad (1973), who investigated the response of shear flow to acoustic excitation at two frequencies simultaneously.

The maximum amount of frequency shift that can be produced by sound indicates the relative sensitivity of the vortex-shedding to acoustic excitation. A *less robust* wake will exhibit broader ranges of lock-in. Although a clear cut definition of lock-in is somewhat subjective, here it will be conservatively defined as when the wake hot-wire spectrum shows the absence of any pronounced peak at f_o. As well, it is convenient to use frequency ratio f_o/f_e, to quantify the mean flow velocity, because it directly gives a measurement of the shift of the vortex-shedding. In the majority of the forced vibration literature, the frequency ratio is defined as the inverse, f_e/f_o, because in these experiments the flow velocity is typically set, fixing f_o, and f_e is then varied. The opposite is done in the present experiments.

Lock-in is associated with the whole wake response and point measurements obtained on the cylinder surface (i.e., dynamic pressure), may not necessarily be indicative of the wake behaviour. Evidence of this can be seen in Fig. 6. The pressure tap spectra shows a larger peak at f_e relative to f_o than in the hot-wire spectra. It is for this reason that lock-in was determined through the use of the wake hot-wire.

Fig. 10 shows the lock-in region for the single cylinder where v_p/U is plotted against f_o/f_e. Sets of wake hot-wire spectra obtained at $f_o/f_e = 1.01$ are also included. This figure shows the effect that increasing the level of the applied sound field has on the vortex-shedding and helps to clarify the definition of lock-in used here. Although it appears that the natural vortex-shedding frequency is at the frequency of excitation, there is no evidence of the applied sound in the spectra until $v_p/U = 1.29\%$. The vortex-shedding is deemed to be locked-in here because the peak begins to shift and narrow to f_e. As v_p/U is further increased, the response narrows and increases in magnitude. It should also be noted that the boundary of the lock-in range in Fig. 10 is only an estimate, because rather than increase the acoustic sound level until lock-in was achieved for each flow velocity, only the six aforementioned acoustic levels were tested for eight mean flow velocity increments. This still is representative of the lock-in envelope, because this represents 56 independent tests including the tests with no applied sound. For the single cylinder the frequency ratio f_o/f_e, was increased in increments of approximately 0.02, although around frequency coincidence the increment was refined to 0.01.

Fig. 11 shows the entrainment envelope again, but here the sample spectra correspond to an acoustic excitation level of $v_p/U = 3.86\%$, and show the effect of changing flow velocity. At $f_o/f_e = 0.94$, there is evidence of excitation in the wake, but the vortex-shedding peak is still pronounced. There is also evidence in this spectrum of a modulation peak at $2f_e - f_o$. At the next highest f_o/f_e shown, the modulation peak disappears and the wake is locked-in. Although the level of acoustic excitation here remains constant, the peak at f_e is much larger than the previous case indicating that the locked-in wake is more dominant. As f_o/f_e is further increased to 1.05, the vortex-shedding peak begins to reestablish itself. Although there is slight evidence of the vortex-shedding peak in the spectra, the flow is considered here to be weakly locked-in, because of the diminished magnitude of the vortex-shedding peak. Here the peak magnitude at f_o is quite small compared to the peak due to vortex-shedding for $f_o/f_e = 1.09$, for example. A further increase in the flow velocity results in increasing f_o beyond f_e, and the peak at f_o reestablishes itself, and the lock-in subsides.

A similar series of tests were performed for the tandem cylinders. These tests covered a much broader range of Reynolds number ($5000 < \mathrm{Re}_D < 24\,000$) because the respective lock-in ranges for these cylinders was found to be significantly larger than for the single cylinder. Fig. 8 shows spectra obtained for the $L/D = 2.5$ tandem cylinder pitch ratio at $f_o/f_e = 0.80$, plotted in the absence and presence of acoustic excitation. It is apparent that applied sound can induce a locked-in wake similar to that of the single cylinder. The major difference is the amount of frequency shift, and this figure shows a shift of 20% from the natural vortex-shedding frequency.

Fig. 9 shows the same tandem cylinder system for $f_o/f_e = 0.69$, when the wake is not locked-in. Spectra with no applied sound and $v_p/U = 1.29\%$ are plotted on top of each other to allow comparisons to be made. Under the influence of acoustic excitation, it is clear from the size of the vortex-shedding peak as measured by the roving hot-wire probe, that the wake is not locked-in, but the flow sensors show evidence of the excitation frequency in the spectra. The vortex-shedding peak is slightly diminished as well. Both hot-wire spectra show peaks at $f_e \pm f_o$ and the downstream pressure tap also shows evidence of frequency modulation at $f_e \pm f_o$. It should be pointed out that the noise floor of the pressure tap spectra, and in particular the upstream pressure tap signal, shows the background noise signature of the wind-tunnel including the blade passing frequency (BPF) of the blower. This is unavoidable due to the relatively small pressure signals measured on the upstream cylinder here. The downstream pressure tap noise floor is considerably *cleaner* because the shear layers reattaching onto the face of the downstream cylinder create a larger signal, although

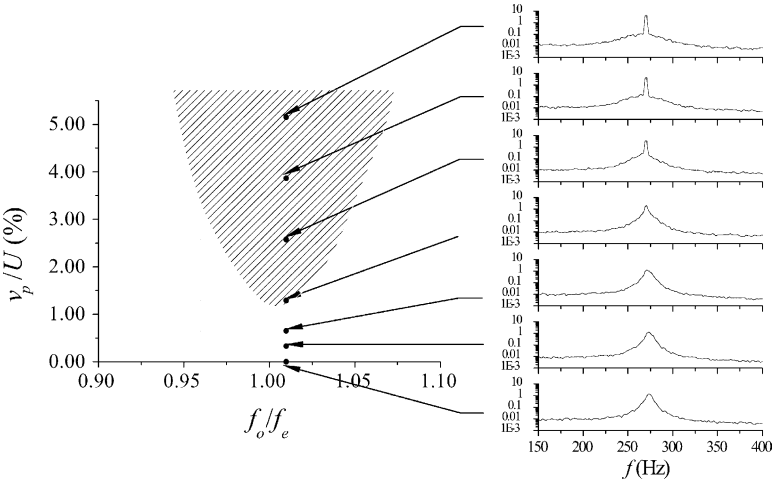

Fig. 10. Entrainment envelope for single cylinder showing effect of changing applied sound amplitude. Spectra obtained with wake hot-wire probe.

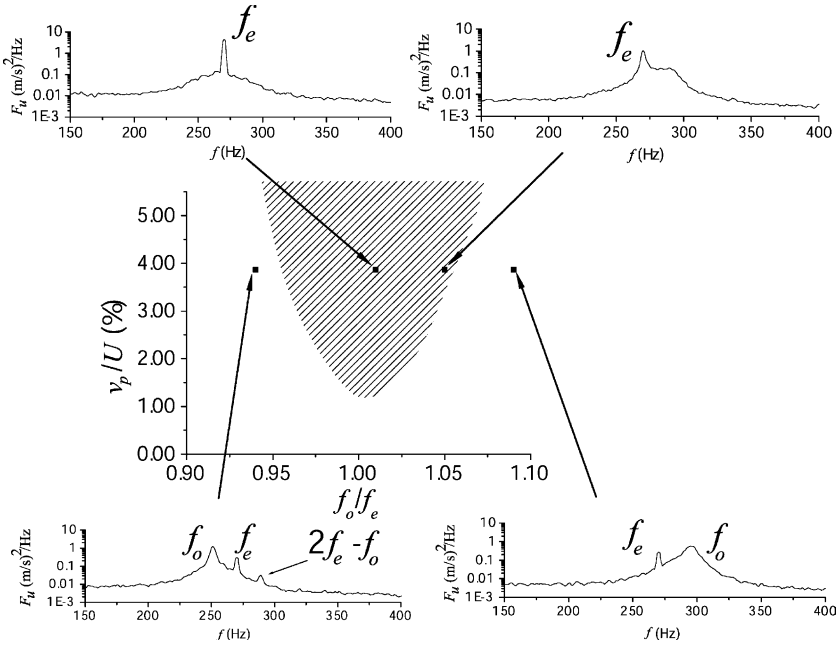

Fig. 11. Entrainment envelope for single cylinder showing effect of changing flow velocity. Spectra obtained with wake hot-wire probe.

there is still slight evidence of background noise in the spectrum. Nonetheless, comparisons between spectra can be made if they are plotted on top of each other as is done in Fig. 9. A nonlinear peak is observed at $f_e + f_o$ in the upstream pressure tap spectrum. Although not shown, the two wake responses shown in Figs. 8 and 9 for this tandem cylinder system are also indicative of the $L/D = 1.75$ case, and represent typical locked-in and modulated wake responses.

Fig. 12 shows the lock-in range for all configurations tested with dimensionless acoustic particle velocity (v_p/U) plotted with respect to frequency ratio. The frequency ratio for the tandem cylinder configurations were increased in increments of approximately 0.02 owing to the much broader range of flow velocities tested than for the single cylinder. It is apparent for the single cylinder that the minimum amplitude required to induce lock-in, the so-called threshold amplitude, was $v_p/U = 1.29\%$. The vortex-shedding could also be shifted off the natural frequency by 4% using the highest v_p/U tested, 5.15%. Both tandem cylinder wakes are considerably more sensitive to acoustic disturbances than the single cylinder wake. For $L/D = 2.5$ and $v_p/U = 5.15\%$, the wake was locked-in for a range of $0.71 < f_o/f_e < 1.10$.

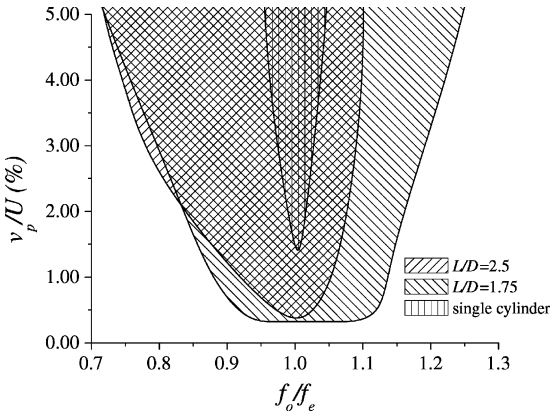

Fig. 12. Experimentally determined lock-in range for single and tandem cylinders using acoustic excitation.

This is significantly larger than the single cylinder range and represents a remarkable frequency shift of almost 30%. The minimum amplitude required to induce lock-in for this tandem cylinder system was for the lowest amplitude tested, $v_p/U = 0.33\%$, and this is substantially lower than the single cylinder threshold amplitude. The $L/D = 1.75$ lock-in range was considerably larger still than either the single cylinder or the tandem cylinder with spacing $L/D = 2.5$. The vortex-shedding could be locked-in for frequency ratios of $0.71 < f_o/f_e < 1.22$. The vortex-shedding seems to be especially receptive at frequency ratios above 1, and the smallest dimensionless acoustic particle velocity tested ($v_p/U = 0.33\%$) entrained the vortex-shedding for a much broader range than either the $L/D = 2.5$ case or the single cylinder.

The present tandem and single cylinder results are compared to the lock-in range reported by Mahir and Rockwell (1996) in Fig. 13 for a tandem cylinder system of pitch ratio $L/D = 2.5$. Mahir and Rockwell's data are plotted in terms of f_e/f_o, and the f_o/f_e values shown in Fig. 13 have been inverted. The forced vibration amplitude A, is nondimensionalized by D, and plotted again against frequency ratio. For the present results, the acoustic particle displacement is also nondimensionalized by the cylinder diameter. The curves plotted in Fig. 13 represent the lower limits of the lock-in range for each configuration tested. It is readily apparent that vortex-shedding is much more sensitive to acoustic disturbances than to cylinder motion. This was also noted by Blevins (1985) for the single cylinder. It also appears the width of the acoustically induced lock-in range for $L/D = 2.5$ is quite similar to the forced-vibration experiment of Mahir and Rockwell (1996) with the same pitch ratio.

Rather than convert the present results to ζ/D, the results of Mahir and Rockwell (1996) shown in Fig. 13 could have similarly been converted to v_c/U, where v_c represents the cylinder velocity. This allows the ratio between the imposed disturbances to be compared, be it acoustic particle velocity or cylinder vibration velocity, relative to the mean velocity. Mahir and Rockwell (1996) found the lowest vibration amplitude that induced lock-in for a single cylinder to be $A/D = 0.10$, at an excitation frequency of 1.33 Hz. Assuming simple harmonic motion, this yields a velocity ratio of $v_c/U = 13\%$. This value is an order of magnitude higher than the lowest acoustic excitation level of $v_p/U = 1.29\%$ required to initiate lock-in in the present single cylinder experiments. For the $L/D = 2.5$ tandem cylinder case, Mahir and Rockwell (1996) report a threshold amplitude of $A/D = 0.05$, this time for $f_e = 0.93$ Hz. A similar analysis yields a velocity ratio of $v_c/U = 5\%$, and again this is significantly higher than the threshold value of $v_p/U = 0.33\%$ for which lock-in was achieved for both tandem cylinder cases. Blevins (1985) noted similar trends in his test of a single cylinder in the presence of sound as well.

Fig. 14 shows a plot of phase angle between the pressure tap on the cylinder and the pressure as on the wind-tunnel wall measured at f_e. In the present work, the pressure tap is oriented at 80° from the front stagnation point. This particular phase was plotted because the pressure tap signal should at least, *loosely*, quantify the phase of the fluctuating lift force on the cylinder. This signal is referenced to the test-section wall microphone signal P_{wall}, which can be related to the acoustic particle displacement by means of Eq. (A.6). This is shown in more detail in Hall (2001). In essence, Fig. 14 relates the fluctuating lift forces to the relative position of the acoustically oscillated fluid, rather than the oscillated cylinder position as is commonly done in forced vibration studies. The phase relationship between P_u and P_{wall} is the same as between fluctuating lift and acoustic particle displacement, ζ.

It is apparent in Fig. 14 that all of the data sets, with the exception of the smallest amplitude tested, exhibit a similar 140° phase jump as flow velocity is passed through frequency coincidence. This is quite similar to the single cylinder forced-vibration results of Bearman and Currie (1979), where phase was measured between the signal from a pressure tap oriented 90° from the front stagnation point referenced to the cylinder displacement. They reported a phase jump of

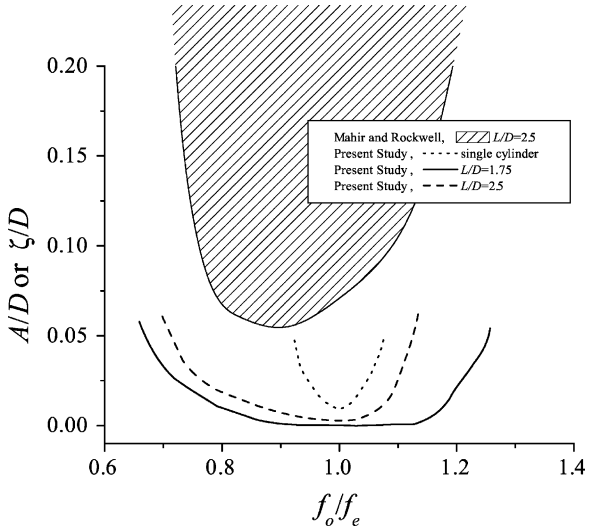

Fig. 13. Experimentally determined acoustically induced lock-in range for single and tandem cylinders compared to tandem cylinder forced vibration experiment. Curves represent lower limit of vortex-shedding entrainment.

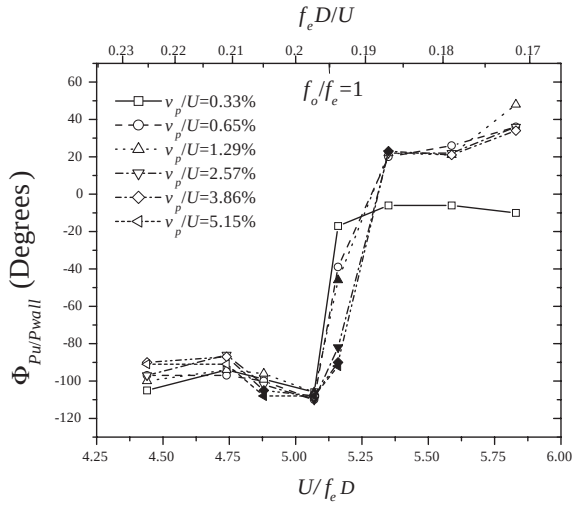

Fig. 14. Variation in phase angle between pressure tap and test-section wall pressure signal with excitation amplitude for a single cylinder. Solid points denote locked-in wake.

approximately 120°. Blevins' phase results, obtained with surface-mounted flush film anemometers referenced to the test-section wall microphone also show a phase jump of approximately 130° as velocity is passed through frequency coincidence. This is commonly interpreted as a change in the timing of vortex-shedding and has been examined in detail by Ongoren and Rockwell (1988) for example.

Efforts were made to employ the measured phase data to relate the phase of the fluctuating lift force on the cylinder to the acoustic particle displacement. The objective was to gain more insight into energy transfer from the mean flow into the acoustic field, and vice versa, and thus assess the effect of frequency ratio on this energy transfer. However, these efforts had to be abandoned because of the uncertainties involved in relating the lift force to a single point measurement of the fluctuating pressure on the surface of the cylinder.

Fig. 15(a) shows a similar plot of the phase relationship between the pressure tap on the upstream cylinder, and the acoustic pressure at the test-section wall for the tandem cylinder configuration with pitch ratio $L/D = 2.5$. Phase is plotted against reduced velocity on the bottom axis, and its inverse, the acoustic Strouhal number $\mathrm{St}_e(L)$ based on spacing L. Locked-in wake states are shown by solid data points. It is apparent there is an approximate 180° phase shift

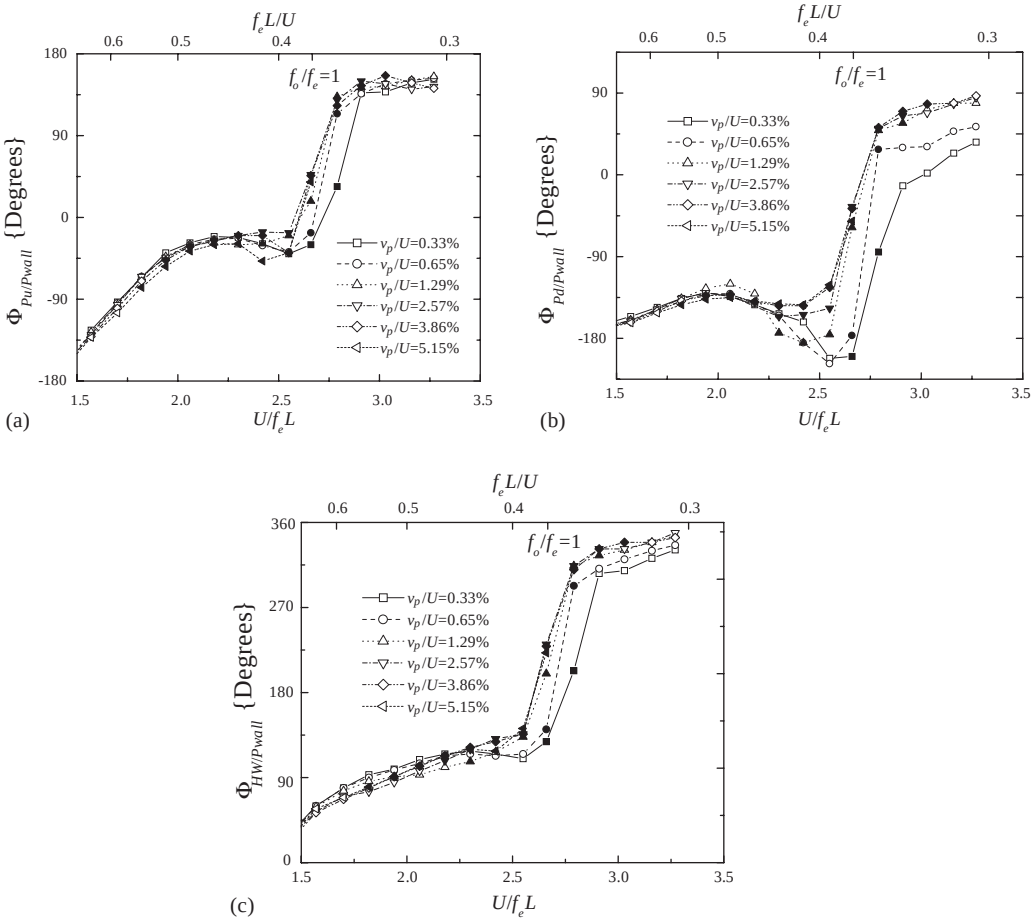

Fig. 15. Variation of phase angle between microphone mounted on test-section wall and (a), upstream pressure tap, (b), downstream pressure tap and (c), stationary hot-wire probe for tandem cylinders with pitch ratio $L/D = 2.5$. Solid points denote locked-in wake.

as velocity is increased through frequency coincidence, similar to the results obtained for the single cylinder. Fig. 15(b) shows a similar plot for the phase difference between the pressure tap on the downstream cylinder, P_d, and the acoustic pressure on the test-section wall. Here, a larger phase jump of approximately 280° occurs at $f_o/f_e = 1$. This larger jump seems to be due to the acoustically induced phase angle reduction before frequency coincidence and is likely at least in part due to the reattachment point of the shear-layers on the face of the second cylinder moving slightly with changes in flow velocity and excitation amplitude. The phase shift measured from the beginning of the lock-in range to the end is observed to be only slightly larger than 180°. To ensure that the observed phase jump is real, and is not just a manifestation of a moving reattachment point, the phase from the stationary hot-wire signal referenced again to P_{wall} shows that the phase jump is indeed a feature of the flow field. The phase jump in velocity fluctuations as frequency coincidence is passed again is on the order of 180°, and qualitatively looks strikingly similar to the case shown in Fig. 15(a). The signal measured by the stationary hot-wire probe is indicative of the enveloped flow by the wake and the gap, although the absolute value of the phase angle for this case likely has little physical meaning. Interestingly, the phase behaviour of this tandem cylinder system is similar to the single cylinder case.

The phase jump depicted in Fig. 15 is also evident from the flow visualization photographs shown in Fig. 16. These photographs were obtained in the wake of the $L/D = 2.5$ case at the same instant of the acoustic cycle at velocities above and below frequency coincidence. It is readily apparent that the timing of the vortex-shedding has changed by approximately 180°. This corroborates the phase measurements shown in Fig. 15 and is consistent with the single cylinder, forced vibration, flow visualization by Ongoren and Rockwell (1988).

The phase plots for the tandem cylinder with pitch ratio $L/D = 1.75$ are shown in Fig. 17 and are markedly different from the aforementioned cases. A plot of the phase angle between P_d and P_{wall} is shown in Fig. 17(a), and it is clear that

there is no phase jump as frequency coincidence is passed. The phase angle increases fairly linearly over the entire lock-in range. The phase angle for the P_u case is not shown because it appears that the measurements were contaminated by the acoustically induced change in separation point. The interested reader is directed to Hall et al. (2002a). To further examine this peculiar phase behaviour, a plot of the phase of the stationary hot-wire signal again referenced to the test-section microphone signal is shown in Fig. 17(b). With the exception of a -140° phase jump before the first lock-in is approached, the phase appears quite similar to the phase of the downstream pressure tap in that the phase seems to increase linearly. The flow visualization performed in the wake of this case also proved inconclusive. The meaning of this behaviour is unclear but seems to suggest some form of convective instability. Ongoren and Rockwell (1988) also noted no phase jump at frequency coincidence for a forced, single square cylinder.

Another interesting feature observed in the aforementioned phase plots concerns the acoustic Strouhal number, $\mathrm{St}_e(L)$ at the onset of the lock-in range for high excitation levels. As shown in Fig. 17, the onset of lock-in occurs at a nearly constant value of $\mathrm{St}_e(L) \sim 0.5$. The same is shown in Fig. 17 for the $L/D = 1.75$ tandem cylinder case. This suggests that the streamwise cylinder spacing is the dominant length scale which determines the acoustic Strouhal number, and consequently the frequency ratio at the onset of lock-in. This notion seems to agree with the observed dominance of the impinging length scale in the excitation mechanisms of flow-excited acoustic resonance for several different flow configurations, such as deep cavities (Ziada, 1994), and heat exchanger tube bundles (Oengören and Ziada, 1992). In fact, Ziada (1998) reported that acoustic resonance of heat-exchanger tube-bundles arranged in

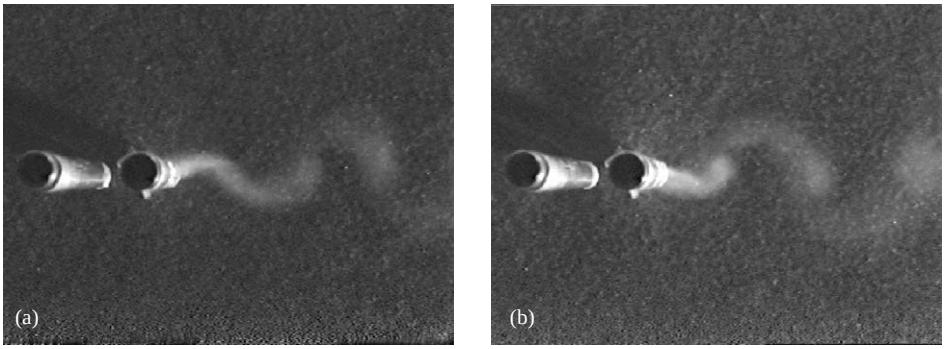

Fig. 16. Flow visualization showing variation in wake timing for tandem cylinders with pitch ratio $L/D = 2.5$ and excitation amplitude $v_p/U = 1.29\%$. For (a), $\mathrm{St}_e(L) = 0.435$, $f_o/f_e = 0.87$, and (b), $\mathrm{St}_e(L) = 0.343$, $f_o/f_e = 1.08$. Photographs are taken at same acoustic instant. Flow is from left to right.

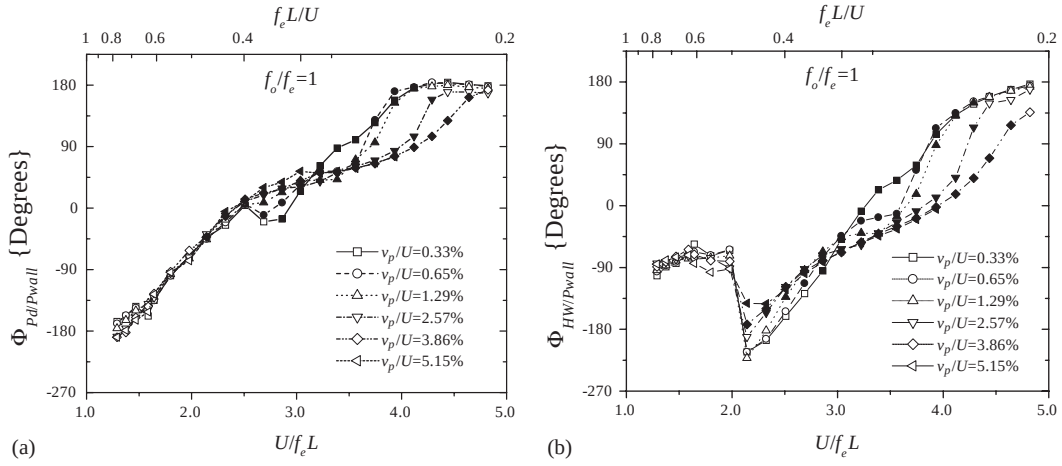

Fig. 17. Variation in phase between test-section microphone and (a), downstream pressure tap and (b), stationary hot-wire probe with flow velocity. Pitch ratio $L/D = 1.75$. Solid points denote lock-in.

approximately square arrays is initiated at a constant Strouhal number based on the streamwise tube spacing, L, and this was also found to occur at $\mathrm{St}_e(L) \sim 0.5$.

Fig. 18 shows flow visualization of the gap flow for each tandem cylinder case performed near frequency coincidence, $f_o/f_e = 0.98$, for high and low levels of excitation. All photographs are taken at the same instant of the acoustic cycle. In the left side of the figure, for low excitation, $v_p/U = 1.29\%$, the wake flow is locked-in and no vortex-shedding is evident in the gap for either pitch ratio. In the right column, however, for high excitation, $v_p/U = 5.15\%$, vortex-shedding is induced in the gap region for the $L/D = 2.5$ case. Although it may be slightly unclear from the photographs, videos obtained show clear periodic vortex-shedding in the gap for this case. It is also clear that no vortex-shedding is noted in the gap region for $L/D = 1.75$, although for high excitation levels at frequency coincidence definite swinging of the gap region was detected. It is likely that vortex-shedding could be induced in the gap for the $L/D = 1.75$ pitch ratio with higher excitation levels, although practically this is difficult because of speaker limitations. If the frequency of applied acoustic excitation is of sufficient amplitude and the vortex-shedding frequency is sufficiently close to the excitation frequency, vortex-shedding may be induced in the gap flow region. Effectively the applied sound lowers the critical spacing. Mahir and Rockwell (1996) reported similar results for the $L/D = 2.5$ case in their forced vibration study. Fundamental changes in flow structure caused by sound are well documented in shear flows (see review by Ho and Huerre, 1984), and has in fact been shown to cause flow regime transitions for cylinders closely mounted in a side-by-side arrangement by Kim and Durbin (1988).

4. Concluding remarks

It is clear that the behaviour of both tandem cylinder arrangements, $L/D = 1.75$ and 2.5, in the presence of an applied sound field is similar to the behaviour of the single cylinder, in that the sound can induce locked-in wake states if the excitation frequency is sufficiently close to the natural vortex-shedding frequency. If the wake is not locked in, but the excitation frequency is sufficiently close to the natural vortex-shedding frequency, the wake exhibits small spectral peaks at linear combinations of the shedding and excitation frequency. The amplitude of the peaks varies depending on the location of the sensor used to measure the vortex-shedding process.

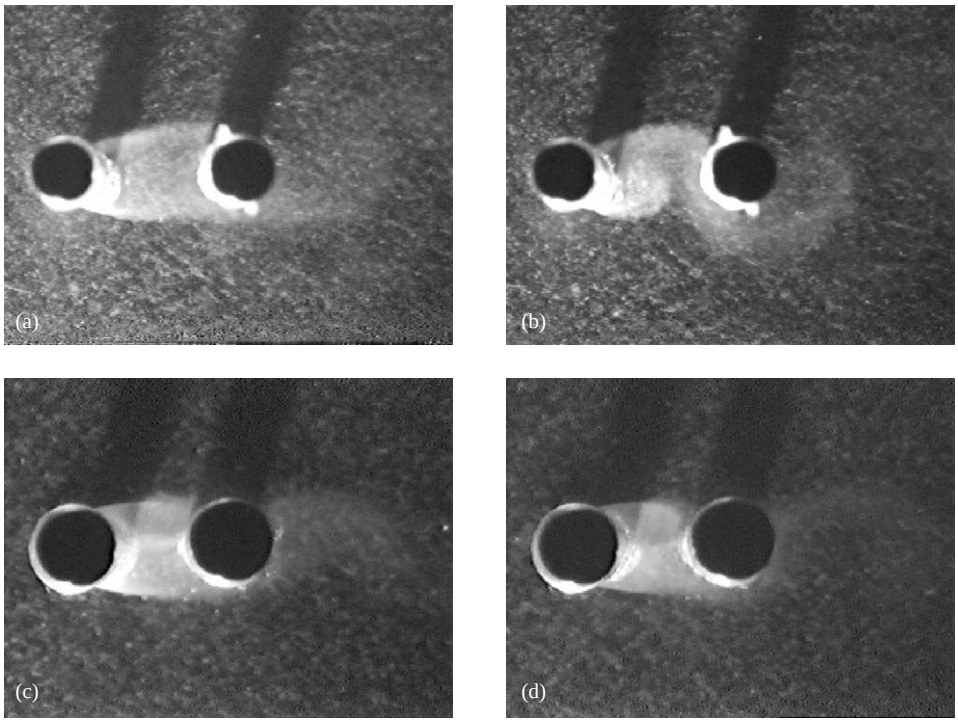

Fig. 18. Flow visualization of the gap flow for tandem cylinders showing variation in amplitude of applied sound field for $L/D = 2.5$, (a), $v_p/U = 1.29\%$ and (b), $v_p/U = 5.15\%$, and for $L/D = 1.75$, (c), $v_p/U = 1.29\%$ and (d), $v_p/U = 5.15\%$. Frequency ratio is $f_o/f_e = 0.98$ and all photos are taken at same point in acoustic cycle. Flow is from left to right.

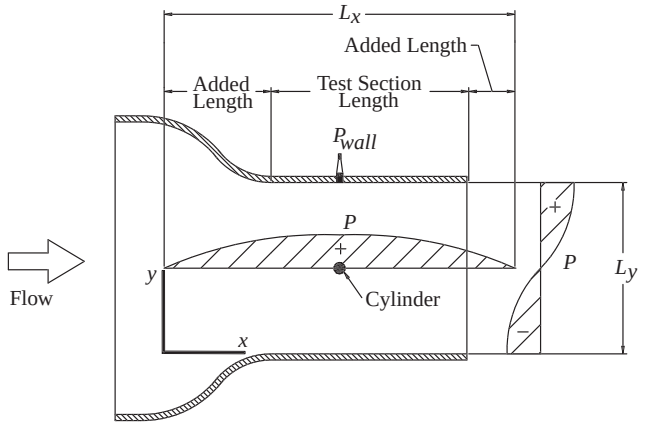

Fig. 19. Pressure wave excited in wind-tunnel test-section.

The relative ease of wake entrainment is not the same for the single cylinder as the tandem cylinder system. The $L/D = 2.5$ case had a lock-in range roughly four times the breadth of the single cylinder range. The tandem cylinder system with pitch ratio $L/D = 1.75$ had a larger lock-in range than either the single cylinder or the $L/D = 2.5$ tandem cylinder configuration, and showed exceptional sensitivity to the lowest acoustic particle velocity tested, $v_p/U = 0.33\%$. Although the present study shows that cylinders in close proximity are extremely *receptive* to acoustic excitation, care should be taken in interpreting these results since this study makes no claims on the *self-excitability* of these systems.

It was shown that when the present results are compared to forced vibration tests, the amplitudes required to produce lock-in are roughly an order of magnitude lower than forced vibration experiments, although both the single cylinder and $L/D = 2.5$ tandem cylinder configuration show comparable changes in the wake timing. The behaviour of the locked-in wake in the presence of an acoustic field appears to be fundamentally the same as for a vibrating cylinder, although the acoustic amplitudes required to produce lock-in are considerably smaller than the forced vibration amplitudes in similar experiments possibly due to differences in the forcing mechanisms. The $L/D = 1.75$ tandem cylinder arrangement did not exhibit a similar change in wake timing and the significance of this is under investigation.

In the present study the sound also promoted vortex-shedding in the gap between the cylinders for the $L/D = 2.5$ case, in effect causing a reduction in the critical spacing. Despite the fact that the $L/D = 1.75$ was extremely receptive to acoustic excitation, no vortex-shedding was observed in the gap for the $L/D = 1.75$ case.

Acknowledgements

The authors gratefully acknowledge the financial support of the Natural Sciences and Engineering Research Council of Canada (NSERC).

Appendix. Acoustic mode

The windtunnel test-section shown in Fig. 19 is considered to behave as an empty duct because of the small diameter of the cylinder. The two-dimensional acoustic mode shapes are given by Kinsler et al. (1982), for example, as

$$p(x, y, t) = P_{\text{wall}} \sin\left(\frac{l\pi x}{L_x}\right) \cos\left(\frac{m\pi y}{L_y}\right) e^{i2\pi f_e t}, \tag{A.1}$$

where P_{wall} is the peak acoustic pressure amplitude recorded by the test-section wall microphone, and l and m are the mode numbers in the x and y directions, respectively. Kinsler et al. (1982) also shows the corresponding acoustic natural frequencies of the section to be

$$f_e = \frac{c}{2} \sqrt{(l/L_x)^2 + (m/L_y)^2}, \tag{A.2}$$

where c is the speed of sound. In the present experiments, the speakers were tuned to excite a persistent and powerful 270 Hz mode in the test-section. Experimental investigation revealed this mode corresponds to $l = 1,\ m = 1$ in Eq. (A.1). This acoustic mode was used because it provided maximum amplification in the test-section. The test cylinders were placed at the streamwise acoustic pressure maximum ($L_x/2$) and the cross-stream acoustic pressure node ($L_y/2$), and the test-section wall microphone was placed at the x location of the cylinders as shown in Fig. 19.

For an acoustic process of small amplitude, Eulers' equation simplifies to

$$\rho \frac{\partial \boldsymbol{v_p}}{\partial t} = -\nabla p, \tag{A.3}$$

where ρ is the ambient density of the fluid. Substituting Eq. (A.1) into Eq. (A.3) and differentiating yields the peak acoustic particle velocity at the cylinder location

$$\boldsymbol{v_p}(L_x/2, L_y/2, t) = -\frac{P_{\text{wall}}}{2\rho L_y f_e} \mathrm{i} e^{\mathrm{i}2\pi f_e t} \hat{\mathbf{y}}, \tag{A.4}$$

for the 270 Hz mode of interest here. Here $\hat{\mathbf{y}}$ represents the unit direction vector in the y direction, normal to the cylinder axis and the mean flow velocity, and i represents the complex number, $\mathrm{i} = \sqrt{-1}$. Inspection of Eqs. (A.1) and (A.4) show that there is a 90° phase lag between v_p and P_{wall}. By definition, acoustic particle displacement is related to acoustic particle velocity by

$$\boldsymbol{v_p} = \frac{\partial \boldsymbol{\zeta}}{\partial t}. \tag{A.5}$$

Hence the acoustic particle displacement at the location of the cylinders is given by

$$\boldsymbol{\zeta}(L_x/2, L_y/2, t) = -\frac{P_{\text{wall}}}{4\pi\rho L_y f_e^2} e^{\mathrm{i}2\pi f_e t} \hat{\mathbf{y}}. \tag{A.6}$$

It is clear from Eqs. (A.4) and (A.6) that there is a 180° phase lag between P_{wall} and ζ, and that there is no acoustic particle motion in the streamwise direction at the position of the cylinders. Since, as Blevins (1985) showed, it is acoustic particle velocity or acoustic particle displacement, rather than acoustic pressure that entrains the vortex-shedding process, the use of the $l = 1,\ m = 1$ pressure wave is effectively the same as exciting with a $l = 0,\ m = 1$ standing wave as done by Blevins.

References

Arie, M., Kiya, M., Moriya, M., Mori, H., 1983. Pressure fluctuations on the surface of two cylinders in tandem arrangement. ASME Journal of Fluids Engineering 105, 161–167.

Bearman, P.W., 1984. Vortex-shedding from oscillating bluff bodies. Annual Review of Fluid Mechanics 16, 195–222.

Bearman, P.W., Currie, I.G., 1979. Pressure fluctuation measurements on an oscillating circular cylinder. Journal of Fluid Mechanics 91, 661–677.

Blevins, R.D., 1985. The effect of sound on vortex-shedding from cylinders. Journal of Fluid Mechanics 161, 217–237.

Feng, C.C., 1968. The measurement of vortex-induced effect in flow past stationary and oscillating circular and D-section cylinders. Masters Thesis, University of British Columbia, Vancouver, British Columbia, Canada.

Hall, J.W., 2001. The effect of applied sound on vortex-shedding from single and tandem cylinders. Masters Thesis, McMaster University, Hamilton, Ontario, Canada.

Hall, J.W., Ziada, S., Weaver, D.S., 2002a. The effect of applied sound on vortex-shedding from single and tandem cylinders. In: CSME Forum, Kingston, Ontario, Canada.

Hall, J.W., Ziada, S., Weaver, D.S., 2002b. The effect of sound on vortex-shedding from single and tandem cylinders. In: Fluid–Structure Interaction, Aeroelasticity, Flow-Induced Vibration and Noise, Paper IMECE2002-32164, ASME, New York.

Ho, C., Huerre, P., 1984. Perturbed free shear layers. Annual Review of Fluid Mechanics 16, 365–424.

Igarashi, T., 1981. Characteristics of the flow around two circular cylinders arranged in tandem (1st report). Bulletin of the JSME 24-188, 323–331.

Kim, H.J., Durbin, P.A., 1988. Investigation of the flow between a pair of circular cylinders in the flopping regime. Journal of Fluid Mechanics 196, 431–448.

Kinsler, L.E., Frey, A.R., Coppens, A.B., Sanders, J.V., 1982. Fundamentals of Acoustics, 3rd Edition. Wiley, Toronto.

Lee, T., Basu, S., 1997. Nonintrusive measurements of the boundary layer developing on single and tandem cylinders. Experiments in Fluids 23, 187–192.

Lee, T., Panagakos, A., 1997. Investigation of boundary layer behavior on single and tandem cylinders. In: Fluid–Structure Interaction, Aeroelasticity, Flow-Induced Vibration and Noise, AD-Vol. 53-1: ASME, New York.

Mahir, N., Rockwell, D., 1996. Vortex formation from a forced system of two cylinders. Part 1: tandem arrangement. Journal of Fluids and Structures 10, 473–489.

Miksad, R.W., 1973. Experiments on non-linear interaction of a free shear-layer. Journal of Fluid Mechanics 59, 1–21.

Norberg, C., 2003. Fluctuating lift on a circular cylinder: review and new measurements. Journal of Fluids and Structures 17, 57–96.

Oengören, A., Ziada, S., 1992. Vorticity shedding and acoustic resonance in an in-line tube bundle. Part 2: acoustic resonance. Journal of Fluids and Structures 6, 293–309.

Ongoren, A., Rockwell, D., 1988. Flow structure from an oscillating cylinder. Part 1. Mechanisms of phase shift and recovery in the near wake. Journal of Fluid Mechanics 191, 197–223.

Zdravkovich, M.M., 1977. Review of flow interference between two circular cylinders in various arrangements. Transactions of the ASME 9, 618–633.

Zdravkovich, M.M., 1987. The effects of interference between circular cylinders in cross flow. Journal of Fluids and Structures 1, 239–261.

Ziada, S., 1994. A flow visualization study of flow-acoustic coupling at the mouth of a resonant side-branch. Journal of Fluids and Structures 8, 391–416.

Ziada, S., 1998. Strouhal numbers of vortex-shedding and acoustic resonance on heat exchanger tube bundles. In: International Symposium on Flow-Induced Vibrations-Horizons, Houston, HTRI (Invited Lecture).